




Lipocalin-2 Is a Key Regulator of Neuroinflammation in Secondary Traumatic and Ischemic Brain Injury

Jae-Hong Kim^{1,2} · Ri Jin Kang^{1,2} · Seung Jae Hyeon³ · Hoon Ryu^{3,4,5} · Hyejin Joo^{6,9} · Youngmin Bu⁷ · Jong-Heon Kim^{2,8} · Kyoungho Suk^{1,2,8} 

Accepted: 28 November 2022 / Published online: 12 December 2022
© The American Society for Experimental Neurotherapeutics, Inc. 2022

Abstract

Reactive glial cells are hallmarks of brain injury. However, whether these cells contribute to secondary inflammatory pathology and neurological deficits remains poorly understood. Lipocalin-2 (LCN2) has inflammatory and neurotoxic effects in various disease models; however, its pathogenic role in traumatic brain injury remains unknown. The aim of the present study was to investigate the expression of LCN2 and its role in neuroinflammation following brain injury. LCN2 expression was high in the mouse brain after controlled cortical impact (CCI) and photothrombotic stroke (PTS) injury. Brain levels of LCN2 mRNA and protein were also significantly higher in patients with chronic traumatic encephalopathy (CTE) than in normal subjects. RT-PCR and immunofluorescence analyses revealed that astrocytes were the major cellular source of LCN2 in the injured brain. *Lcn2* deficiency or intracisternal injection of an LCN2 neutralizing antibody reduced CCI- and PTS-induced brain lesions, behavioral deficits, and neuroinflammation. Mechanistically, in cultured glial cells, recombinant LCN2 protein enhanced scratch injury–induced proinflammatory cytokine gene expression and inhibited *Gdnf* gene expression, whereas *Lcn2* deficiency exerted opposite effects. Together, our results from CTE patients, rodent brain injury models, and cultured glial cells suggest that LCN2 mediates secondary damage response to traumatic and ischemic brain injury by promoting neuroinflammation and suppressing the expression of neurotropic factors.

Keywords Astrocyte · Microglia · Neuroinflammation · Lipocalin-2 · Traumatic brain injury

✉ Kyoungho Suk
ksuk@knu.ac.kr

Jae-Hong Kim
kim86217@nate.com

Ri Jin Kang
flws2001@naver.com

Seung Jae Hyeon
sjhyeon@kist.re.kr

Hoon Ryu
hoonryu@kist.re.kr

Hyejin Joo
joosh561@naver.com

Youngmin Bu
ymbu@khu.ac.kr

Jong-Heon Kim
jongheonkim@knu.ac.kr

² Department of Pharmacology, School of Medicine, Kyungpook National University, Daegu, Republic of Korea

³ Center for Neuroscience, Brain Science Institute, Korea Institute of Science and Technology, Seoul, Republic of Korea

⁴ Veterans Affairs Boston Healthcare System, Boston, MA, USA

⁵ Boston University Alzheimer's Disease Center and Department of Neurology, Boston University School of Medicine, Boston, MA, USA

⁶ Department of Science in Korean Medicine, Graduate School, Kyung Hee University, Seoul, Republic of Korea

⁷ Department of Herbal Pharmacology, College of Korean Medicine, Kyung Hee University, Seoul, Republic of Korea

⁸ Brain Science & Engineering Institute, Kyungpook National University, Daegu, Republic of Korea

⁹ Present Address: Pharmacological Research Division, Toxicological Evaluation and Research Department, Ministry of Food and Drug Safety, National Institute of Food and Drug Safety Evaluation, Chungju, Republic of Korea

¹ Brain Korea 21 Four KNU Convergence Educational Program of Biomedical Sciences for Creative Future Talents, School of Medicine, Kyungpook National University, Daegu, Republic of Korea

Introduction

Traumatic brain injury (TBI), whereby mechanical forces on the head disrupt brain physiology and structure, is a leading cause of hospital utilization and disability worldwide [1–4]. TBI is associated with an increased risk of psychiatric comorbidities [5–7] and neuropathology [8–10] that present and persist beyond the acute post-injury window. Positron emission tomography and post-mortem studies have shown that glial reactivity persists for over a decade after injury [11–14]. Thus, clinical innovation will require the understanding of how processes initiated at impact (primary injury) progress into long-term inflammation and neurodegeneration (secondary injury). Secondary injury is an indirect result of destructive immunological, inflammatory, neurotoxic, and biochemical cascades that are triggered by primary injury [15]. Although some neurological damage is caused by the primary injury, it is increasingly recognized that secondary inflammatory processes have an important pathological role [16]. However, the exact roles of neuroimmune and neuroinflammatory responses in the pathophysiological processes of secondary injury in TBI are largely unknown.

Neuroinflammation is a major pathological process in the secondary response after brain injury [17]. Neuroinflammatory responses in TBI are characterized by glial cell activation and upregulation of inflammatory mediators, which can have both beneficial and detrimental effects [18–21]. Resident immune cells in the central nervous system (CNS), such as astrocytes and microglia, are activated and subsequently form an area of containment between injured and healthy tissues, suggesting that acute activation of glial cells may represent the first line of defense following TBI [20, 22]. However, when glial cells become over-activated, they can induce detrimental neurotoxic effects by releasing cytotoxic molecules, such as proinflammatory cytokines and reactive oxygen and nitrogen species [20, 23]. These inflammatory mediators can further activate glial cells, significantly affecting the pathophysiology of TBI [24]. Thus, the intensity and duration of neuroinflammatory responses are critical in determining their destructive effects on the CNS after TBI.

Lipocalin-2 (LCN2) has been implicated in the regulation of diverse cellular processes such as cell differentiation, apoptotic cell death, and cellular uptake of iron [25, 26]. We first reported that brain glial cells express LCN2, which may in turn regulate their own activation [27–31]. Under inflammatory and pathological conditions, LCN2 plays a critical role as a chemokine inducer [32] and mediator of neuronal cell death [33]. LCN2 has been linked to an experimental autoimmune encephalomyelitis model of multiple sclerosis [34], chronic inflammatory pain [35],

neuropathic pain [36], Alzheimer's disease [37], Parkinson's diseases [38], and vascular dementia [39]. Moreover, previous studies have shown that LCN2 expression is increased in the brain following ischemic stroke [40], intracerebral hemorrhage [41], and stab wound injury [32], suggesting that an increase in LCN2 levels may be related to diverse forms of brain injury [25]. Although a few studies have reported serum and brain LCN2 levels in TBI patients [42, 43], the expression and function of LCN2 in TBI brains are poorly understood.

In the present study, we utilized postmortem brain tissues of chronic traumatic encephalopathy (CTE) patients and mouse models of brain injury induced by controlled cortical impact (CCI) and photothrombotic stroke (PTS) to study the expression and role of LCN2 in traumatic and ischemic brain damage. Here, we report that astrocytic LCN2 mediates neuroinflammatory pathways that contribute to secondary brain injury in CCI and PTS models, as well as in patients with TBI.

Methods

Animals

Male wild-type (WT) C57BL/6 mice (aged 8–12 weeks) were obtained from Samtako (Osan, Republic of Korea), and *Lcn2*-knockout (KO) C57BL/6 mice (aged 8–12 weeks) were kindly provided by Dr. Kiyoshi Mori (Kyoto University, Kyoto, Japan) and Dr. Shizuo Akira (Osaka University, Osaka, Japan). All animal experiments were performed in accordance with approved animal protocols and guidelines established by the Animal Care Committee of Kyungpook National University (No. KNU 2022–0290). Mice were selected randomly for inclusion into various experimental groups, with the researchers performing experimental procedures blinded as to the identity of experimental groups.

Animal Model of TBI

CCI injury was induced as previously described [44]. The mice were anesthetized with 2–5% isoflurane and placed in a stereotaxic frame. A 4-mm diameter craniotomy window was created over the right hemisphere, centered 1.5 mm lateral from the midline. The bone flap was removed to expose the dura mater, and a CCI injury was delivered to the animals in the TBI group using an electromagnetically driven impactor (Impact One Stereotaxic Impactor for CCI, Leica Microsystems, Wetzlar, Germany) with a cylindrical, 2.5-mm diameter tip. The impact parameters were as follows: impact velocity, 2 m/s; penetration depth, 2.5 mm; and dwell time, 300 ms. Sham animals received identical anesthesia

and craniotomy; however, the injury was not induced. After the impact or sham procedure was completed, the bone flap was replaced over the craniotomy window and the scalp was sutured. The CCI-induced mRNA expression in the brain was measured by reverse transcription polymerase chain reaction (RT-PCR) at 24 h and 7–14 days after impact. Immunohistochemistry analyses were performed 7 days after impact. Behavioral tests were performed 6–7 days after impact.

Reverse Transcription Polymerase Chain Reaction

Total RNA was extracted from contralateral and ipsilateral brain tissues or cultured cells using the QIAzol reagent (QIAGEN), according to the manufacturer's protocol. For conventional RT-PCR, reverse transcription was conducted using Superscript II (Invitrogen) and oligo(dT) primers. PCR amplification using specific primer sets was carried out at an annealing temperature of 55–60 °C for 20–30 cycles. PCR was performed using the C1000 Touch Thermal Cycler (Bio-Rad, Foster City, CA). For analysis of PCR products, 10 µl of each PCR was electrophoresed on 1% agarose gel and detected under UV light. Quantitative RT-PCR (qPCR) assay was performed using the one-step SYBR[®] PrimeScript[™] RT-PCR kit (Perfect Real Time; Takara Bio Inc., Tokyo, Japan) according to the manufacturer's instructions, followed by detection using the ABI Prism[®] 7000 sequence detection system (Applied Biosystems, Foster City, CA). Relative changes in gene expression determined by the qPCR were calculated using the $2^{-\Delta\Delta CT}$ method [45]. The primers used for RT-PCR analyses of mouse *Lcn2*, *Tnf*, *Il1b*, *Gdnf*, and *Gapdh* were as follows: *Lcn2*, 5'-ATG TCA CCT CCA TCC TGG TC-3' (forward), 5'-CAC ACT CAC CAC CCA TTC AG-3' (reverse); *Tnf*, 5'-CAT CTT CTC AAA ATT CGA GTG ACA A-3' (forward), 5'-ACT TGG GCA GAT TGA CCT CAG-3' (reverse); *Il1b*, 5'-AGT TGC CTT CTT GGG ACT GA-3' (forward), 5'-TCC ACG ATT TCC CAG AGA AC-3' (reverse); *Gdnf*, 5'-GCA CCC CCG ATT TTT GC-3' (forward), 5'-AGC TGC CAG CCC AGA GAA TT-3' (reverse); and *Gapdh*, 5'-TGG GCT ACA CTG AGG ACC AG-3' (forward), 5'-GGG AGT TGC TGT TGA AGT CG-3' (reverse).

Immunofluorescence Staining

The animals were anesthetized using diethyl ether and transcardially perfused first with saline and then with 4% paraformaldehyde diluted in 100 mM PBS. The brains were fixed in 4% paraformaldehyde for 3 days and then cryoprotected using a 30% sucrose solution for an additional 3 days. The fixed brains were embedded in OCT compound (Tissue-Tek, Sakura Finetek, Tokyo, Japan) and sectioned into 20-µm-thick slices. For double or triple immunofluorescence analysis,

tissue sections were incubated with mouse anti-GFAP (BD Biosciences, San Diego, CA, Catalog number: 556330), rabbit anti-GFAP (Dako, Glostrup, Denmark; Catalog number: Z0334), rabbit anti-Iba-1 (Wako, Osaka, Japan, Catalog number: 019–19,741), goat anti-Iba-1 (Novus Biologicals, Centennial, CO, Catalog number: NB100-1028), rabbit anti-NeuN (Millipore, Catalog number: ABN78), and goat anti-LCN2 (R&D systems, Minneapolis, MN, catalog number: AF1857) antibodies. Sections were visualized by incubation with Cy3- and FITC-conjugated anti-mouse, rabbit, or goat IgG antibodies (The Jackson Laboratory, Bar Harbor, ME; Cy3-mouse; catalog number: 715–165-151, Cy3-rabbit; catalog number: 711–165-152, Cy5-rabbit; catalog number: 711–175-152, FITC-rabbit; catalog number: 711–096-152, FITC-goat; catalog number: 705–095-147) and examined under a fluorescence or confocal microscope. Fluorescence intensities were quantified using ImageJ software version 1.44 (National Institutes of Health (NIH)). For quantitative analysis, images were obtained from three non-overlapping fields within the ipsilateral brain area.

Human Brain Tissues

Neuropathological processing of normal and CTE human brain samples was performed according to procedures previously established by Boston University's CTE Center. Institutional review board approval for ethical permission was obtained from the CTE Center [46, 47]. This study was reviewed by the Boston University School of Medicine Institutional Review Board (Protocol H-28974) and was approved as an exemption because the study involved only tissue collected from postmortem individuals, which are not classified as human subjects. The next of kin provided informed consent for participation and brain donation. The study was performed in accordance with the institutional regulatory guidelines and the principles of human subject protection within the Declaration of Helsinki. All participant characteristics are summarized in Supplementary Table 1.

Immunohistochemistry Analysis of Human Postmortem Brain Tissue

LCN2 Staining Paraffin-embedded tissues were sectioned in a coronal plane at 10 to 20 µm as previously described [48]. The tissue sections were rehydrated, blocked with blocking solution (1% H₂O₂), and incubated with goat polyclonal antibody to LCN2 (1:200 dilution; R&D Systems, catalog number: AF1857) for 24 h. After washing three times, the slides were processed with Vector ABC Kit (Vector Laboratories, Inc., Burlingame, CA). The immunoreactive signals were developed with DAB chromogen (Thermo Fisher Scientific, Meridian, Rockford, IL).

GFAP Staining Endogenous alkaline phosphatase was blocked using 3% H₂O₂ in TBS. Sections were blocked with 2.5% normal horse serum (Vector Laboratories) before incubation for 24 h with a rabbit polyclonal anti-GFAP antibody (1:200 dilution; Sigma Aldrich, catalog number: AB5804). After washing, the sections were incubated with ImmPRESS-AP anti-rabbit IgG (alkaline phosphatase) polymer detection reagent (Vector Laboratories) for 30 min at room temperature. Colors were developed using a Vector Red Alkaline Phosphatase Substrate Kit (Vector Laboratories). Slides were subsequently counterstained with hematoxylin (Vector Laboratories), and processed back to xylene using an increasing ethanol gradient (70%, 80% and 95% (1 time), and 100% (2 times)) and then mounted. Images were analyzed using a bright field microscope.

Image Analysis of Human Tissue Sections

Semi-quantitative assessment of immunohistochemistry signals and co-localization patterns was performed using CellSens Imaging Software (Olympus Korea Co.). Co-localized areas (regions of interest) in merged images from two overlapping chromogenic dyes were selected by drawing a transverse line. The signal intensity of interest on the selected line was automatically calculated by the software module and transferred to a Microsoft Excel file to generate statistics and representative graphs. To measure the morphological and structural change of GFAP-positive astrocytes, we performed Sholl analysis using bright-field images immunostained with GFAP antibody. The image of the GFAP immunoreactivity in the cortex was adopted for analysis. In brief, the Sholl analysis manually draws serial concentric circles at 5- μ m intervals from the center of the GFAP-positive astrocyte to the end of the most distant process in each single astrocyte, and analyzes the number of intersections of GFAP processes in each circle. The Sholl analysis was done by using NIH ImageJ software (version 1.44).

RNA Sequencing

To determine human *LCN2* mRNA levels, RNA sequencing data (European Nucleotide Archive database under accession no. ERP015139) from normal postmortem brains and those with CTE were analyzed [49]. Relative *LCN2* mRNA levels were calculated as fold changes in fragments per kilobase of exon per million reads.

Quantification of Brain Lesion Volume

Brain damage was visualized using Cresyl violet staining. Frozen sections were cut (20 μ m thick) in the coronal plane and thaw-mounted onto Superfrost plus slides. Sections were stored at -20 °C. Cresyl violet staining was performed to

delineate brain damage as follows. Cresyl violet staining images were obtained. The lesion was clearly delineated as a region of pallor within the injured brain. A calibration standard was used for each image. The assessor outlined the damaged area using Image J (NIH, version 1.41) on nine standard coronal planes from each brain. The damage volumes were derived by calculating the average damage area between the slices and multiplying it by the distance between the slices. Edema corrections were calculated by dividing the ipsilateral hemisphere volume by the contralateral hemisphere volume.

Behavioral Testing

Pole Test The pole test was performed by modifying the method described by Abe et al. [50]. Mice were positioned head downwards near the top of a rough-surfaced wood pole (10 mm in diameter and 50 cm in height), and the time taken for the mice to reach the floor was recorded. The test was repeated three times at 30-s time intervals, and behavioral changes were evaluated according to the average of the three descending times.

Adhesive Removal Test The adhesive removal test was performed as previously described, with slight modifications [51]. Two adhesive tapes (0.3 \times 0.4 cm²) were applied with equal pressure on each animal paw. The mouse was then placed in a Perspex box, and the time to contact and remove each adhesive tape was recorded, with a maximum of 120 s.

Y-maze Test The Y-maze test was conducted as previously described with slight modifications [52]. Spatial cognition was evaluated using a spontaneous alternation task in the Y-maze apparatus. The Y-maze is a three-arm horizontal maze (40 cm long and 3 cm wide, with 12-cm high walls) in which the arms are at 120° angle to each other. Animals were initially placed within the center, and the sequence and number of arm entries were recorded manually for each animal over a 7-min period. Spontaneous alternation was defined as entry into all three arms upon consecutive choices. The maze arms were thoroughly cleaned with water between and after the consecutive placement of the animals to remove residual odors. The total number of arm entries was used as an indicator of locomotor activity.

Passive Avoidance Test The passive avoidance test was conducted as previously described with slight modifications [53]. This test began with training in which a mouse was placed in a light chamber; when the mouse crossed over to the dark chamber, it received a mild (0.25 mA/s) electric shock on the foot. The initial latency to enter the dark (shock) compartment was used as a baseline measure. During the probe trials, 24 h after training, the mouse was again

placed in the light compartment and the latency to return to the dark compartment was measured as an index of passive fear avoidance.

Cylinder Test The cylinder test was conducted as previously described with slight modifications [54]. To perform this test, mice were placed individually in a transparent cylinder (11.5-cm diameter) and video recorded for 5 min to record the laterality of forelimb use of the animals when exploring the cylinder wall. A mirror was placed behind the cylinder at an angle to allow recording of the forelimb movements along 360°. The videos were analyzed in slow motion and frame-by-frame to score the rears, and the number of wall contacts performed independently with the left and right forepaws was counted to a total number of 20 wall contacts per mouse and per session.

Animal Model of Ischemic Brain Injury

A PTS model was used to assess cerebral ischemic injury. The animals were anesthetized using isoflurane. Rose Bengal was injected intraperitoneally at a dose of 100 mg/kg body weight. After 10 min, a green light laser (540 nm, 20 mW) giving an illumination with 2-mm diameter was positioned on the sensorimotor cortex (1.5 mm right from bregma) through the intact skull for 20 min. The PTS-induced protein and mRNA expression in the brain was measured by Western blot and RT-PCR at 0, 3, 18, 24, 48, and 72 h after laser illumination. Immunohistochemistry analyses were performed 3 days after illumination. Behavioral tests were performed 2–3 days after illumination.

Western Blot Analysis

The tissues were lysed in ice-cold RIPA lysis buffer (Thermo Fisher Scientific, Waltham, MA). Protein concentrations in the tissue lysates were determined using the Pierce™ BCA assay kit (Thermo Fisher Scientific). Equal amounts of protein were separated by 12% SDS-PAGE and transferred to polyvinylidene difluoride membranes (Bio-Rad, Hercules, CA). Membranes were blocked using 5% skim milk and incubated sequentially with the following primary antibodies: goat anti-LCN2 antibody (R&D Systems), mouse anti- α -tubulin antibody (Sigma-Aldrich), and the following horseradish peroxidase-conjugated secondary antibodies: anti-goat IgG antibody (Santa Cruz Biotechnology) and anti-mouse IgG antibody (Thermo Fisher Scientific). The blots were developed with ECL Western blotting detection reagents (Thermo Fisher Scientific) and analyzed using the Amersham™ ImageQuant™ 800 biomolecular imager system (General Electric, Boston, MA). Full and uncropped western blotting bands were uploaded as “Supplementary Material-Original Western Blotting Bands.”

Cell Cultures

Mixed glial culture (MGC) was obtained as previously described with some modifications for the present study [55]. Whole brains of mice (3 days old) were chopped and mechanically disrupted using a nylon mesh. The cells obtained were seeded in culture flasks and grown at 37 °C in a 5% CO₂ atmosphere in Dulbecco's modified Eagle's medium (DMEM) supplemented with 10% fetal bovine serum (FBS) and 100 U/ml penicillin–streptomycin. Culture media were changed initially after 7 days and then every 3 days, and cells were used after being cultured for 14–21 days. For WT or *Lcn2*-KO astrocyte cultures, MGC was mechanically agitated at 200 rpm overnight. The culture media containing cells that were detached from the substratum were discarded, and astrocytes were dissociated using trypsin–EDTA (Invitrogen) and then collected by centrifugation at 1200 rpm for 10 min. Primary astrocytes were cultured in DMEM supplemented with 10% FBS and penicillin–streptomycin. Primary microglia were obtained from MGC using a mild trypsinization method [56] and maintained in DMEM supplemented with 10% FBS and penicillin–streptomycin. For the co-cultures of microglia and astrocytes, the cells were mixed and incubated for 48 h.

Intracisternal Injection of LCN2 Neutralizing Antibody

After anesthetization with isoflurane, mice were placed in a stereotaxic apparatus (Kopf Instruments, Tujunga, CA). An incision was made on the scalp by using an operating microscope. Median dissection of the neck muscles exposed the atlanto-occipital membrane that covered the cisterna magna. Using a 30G Hamilton syringe, within 30 s, 5 μ g of LCN2 monoclonal antibody (R&D systems, Minneapolis, MN, catalog number: MAB1857) or isotype IgG control antibody (R&D systems, catalog number: MAB006) was injected into the cisterna magna of mice after CCI injury. The syringe was left in place for 5 min and then removed. To avoid leakage, the atlanto-occipital membrane was immediately covered with a tissue adhesive. The skin was closed using 4–0 absorbable sutures.

Scratch Injury Model

The scratch injury was performed as an in vitro model of TBI [57]. Briefly, confluent cell cultures were manually scratched using a sterile pipette tip (200 μ L), which produced a linear tear across the culture wells. In each well of the 6-well culture plates, 4 \times 4 scratches were induced, producing a 3-mm grid. Non-scratched cells were used as the controls. The cells were exposed to PBS, recombinant LCN2 protein, or LCN2 antibody for 72 h after scratch injury.

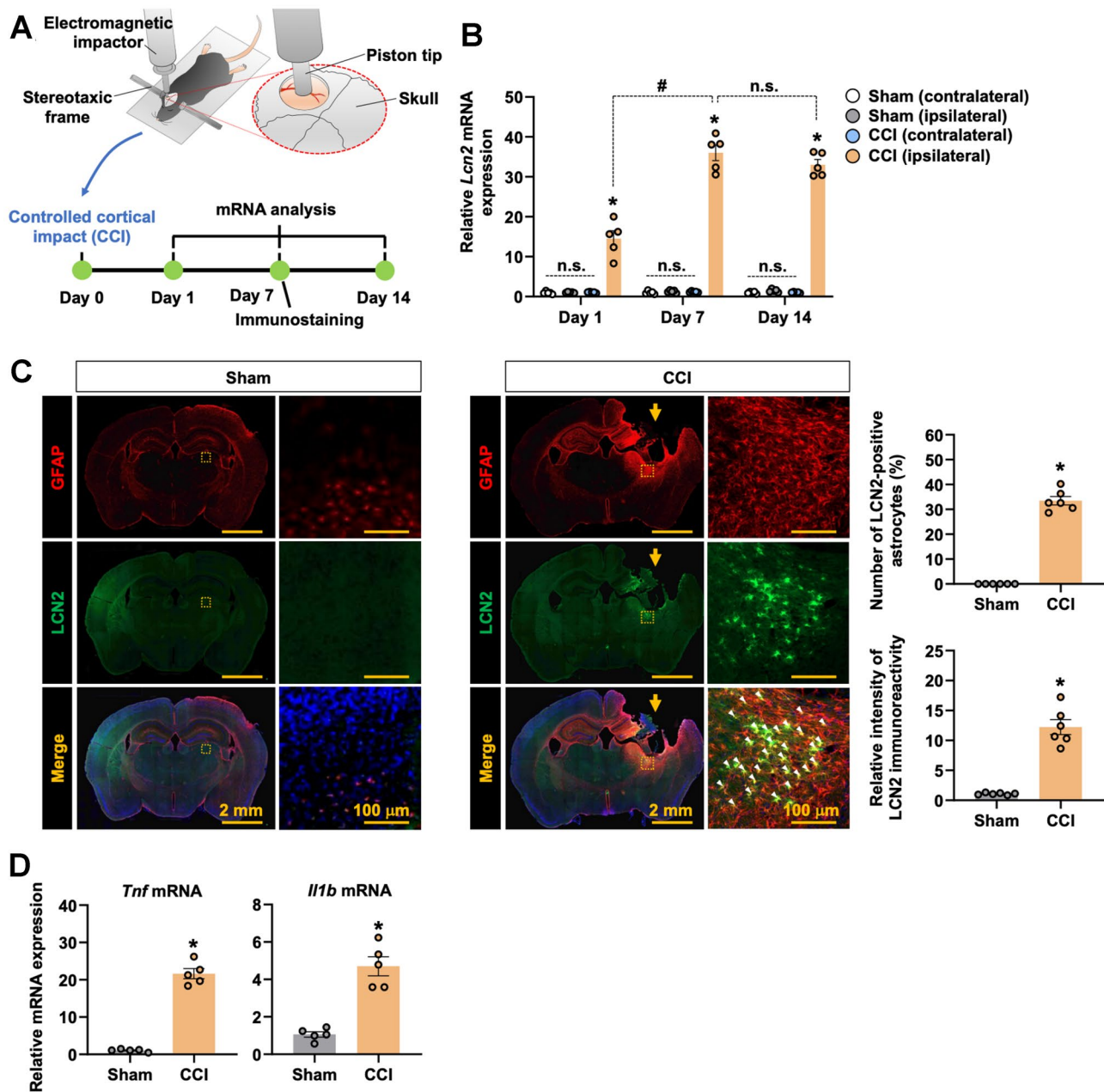


Fig. 1 Induction of LCN2 expression in mouse brain following controlled cortical impact injury. **A** Experimental timeline. **B** The expression of *Lcn2* mRNA in the injured brain at days 1, 7, and 14 following controlled cortical impact (CCI) injury as assessed by qPCR. The mRNA expression profiles are displayed as the fold increase of gene expression normalized to *Gapdh* ($n=5$). * $p < 0.05$ versus sham groups (ipsilateral side); # $p < 0.05$ between the indicated groups; n.s., not significant (one-way ANOVA followed by Tukey's post-hoc test). **C** Immunofluorescence staining of LCN2 in the brain at day 7 after CCI injury. The expression of LCN2 (green) was markedly induced in GFAP-positive astrocytes (red) in injured brain area (ipsilateral).

Nuclei were stained with DAPI (blue). Scale bar, 2 mm or 100 μ m. White arrowheads indicate co-localization of LCN2 and GFAP. Yellow arrows indicate ipsilateral brain. High magnification images corresponding to the dotted square are shown on the right. Quantification of LCN2 immunoreactivity or LCN2-positive astrocytes is shown in the adjacent graphs (right) ($n=6$). **D** The expressions of *Tnf* and *Il1b* mRNA in the injured brain at day 7 following CCI injury were assessed by qPCR. The mRNA expression profiles are displayed as the fold increase of gene expression normalized to *Gapdh* ($n=5$). Results are expressed as mean \pm SEM. * $p < 0.05$ versus sham groups (Student's *t*-test)

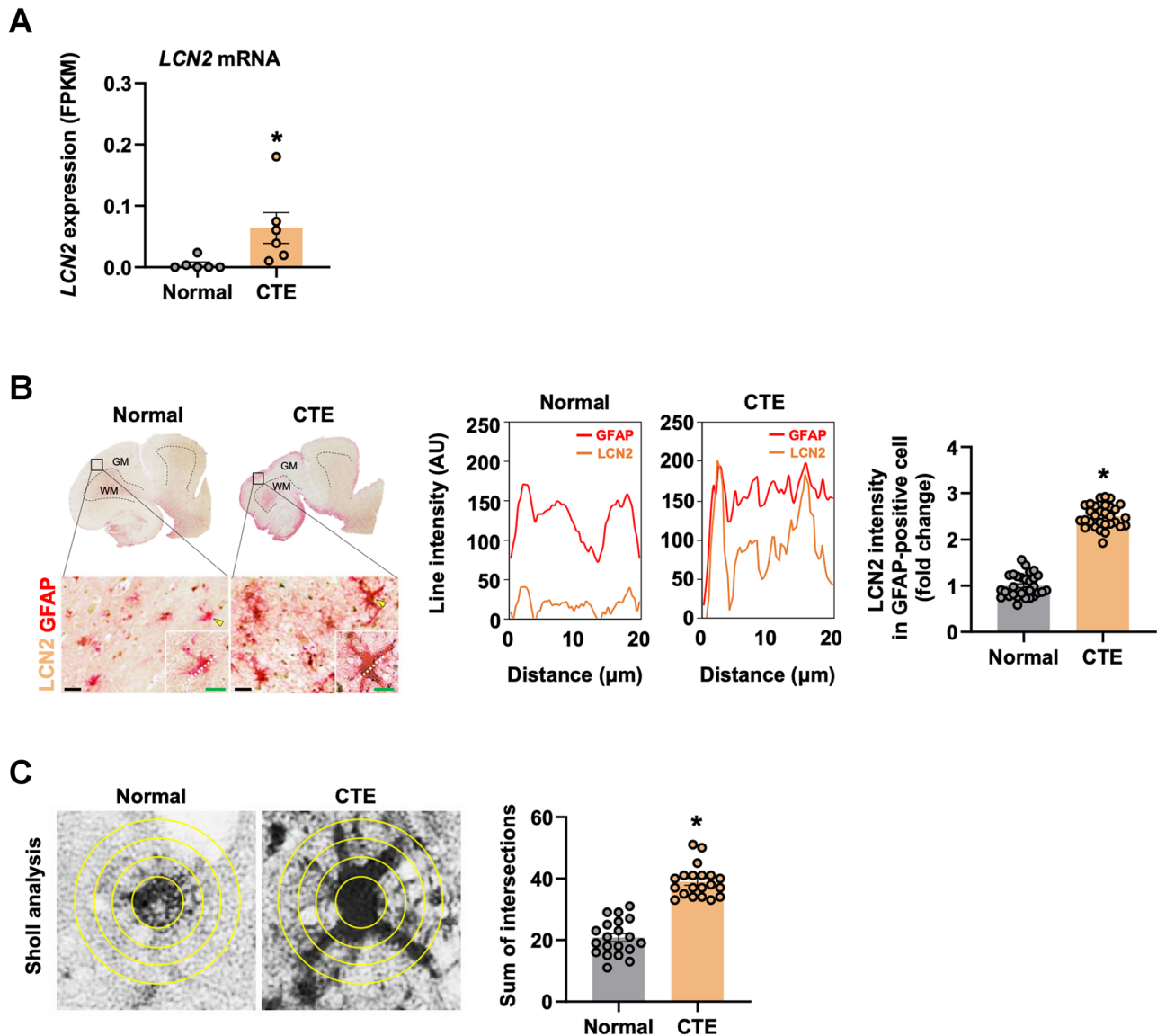


Fig. 2 Upregulation of LCN2 expression in the brain of patients with chronic traumatic encephalopathy. **A** Comparison of LCN2 mRNA expression in the normal and chronic traumatic encephalopathy (CTE) patient brain based on RNA-seq data ($n=6$). **B** Human LCN2 immunoreactivity in GFAP-positive astrocytes of normal controls and patients with CTE (red, GFAP; brown, LCN2). LCN2 was detected using anti-LCN2 antibody and DAB chromogen. GFAP was detected using anti-GFAP antibody and a red alkaline phosphatase substrate kit. GM, gray matter; WM, white matter. Yellow arrowheads indicate the cell magnified in the inset. Scale bars: 20 μm (black) and 10 μm

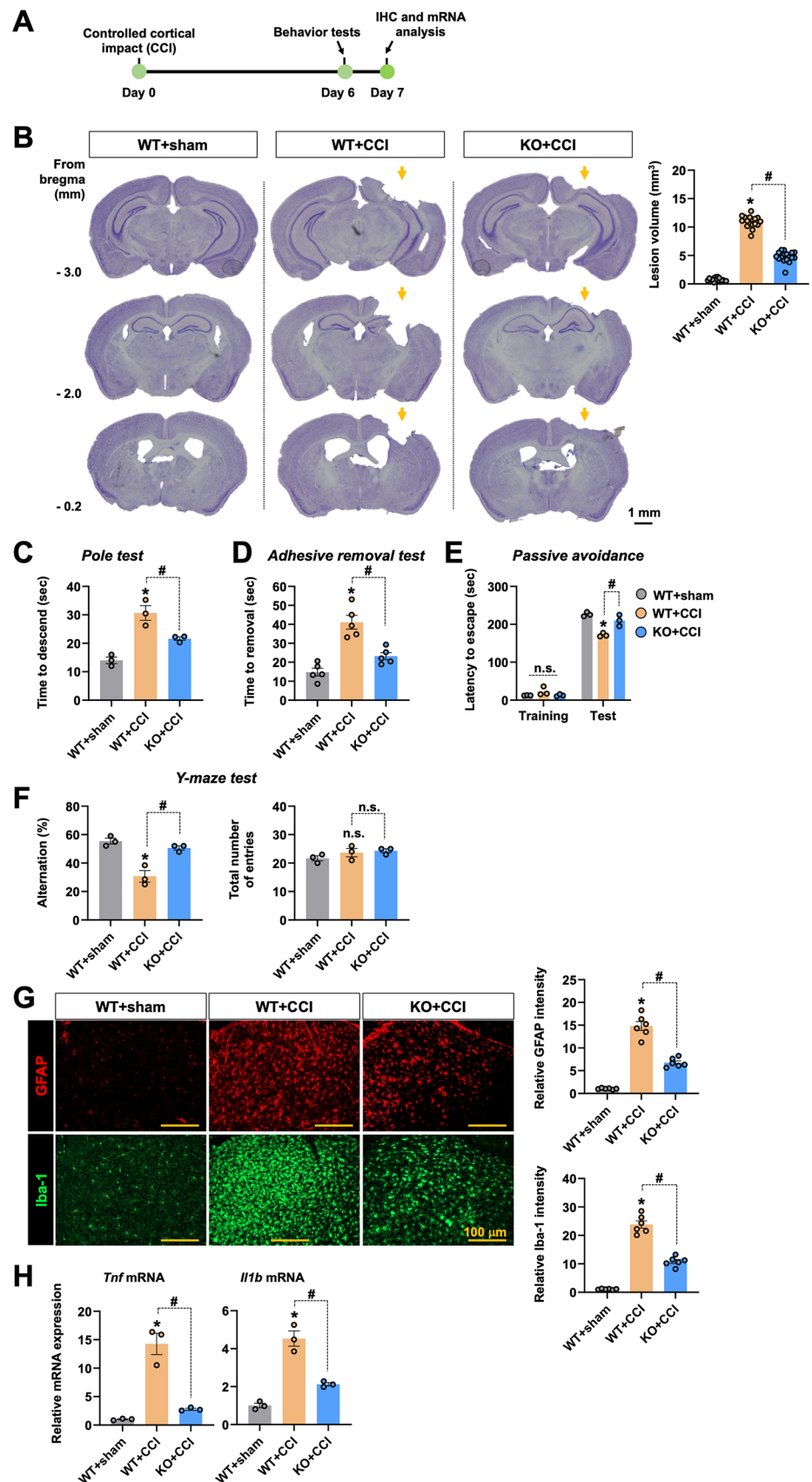
(green). Image analysis: LCN2 signal (brown line) was elevated in GFAP-positive astrocytes (red line) in the cortical region of patients. Quantification of LCN2 intensity in GFAP-positive astrocytes is shown in the adjacent bar graph ($n=30$). **C** Sholl analysis for immunostained GFAP signals. Starting radius, 10 μm ; interval between each concentric circle, 5 μm . The sum of intersections of immunostained GFAP signals crossing the concentric circles is shown in the adjacent bar graph ($n=20$). Results are expressed as mean \pm SEM. * $p < 0.05$ versus normal groups (Student t -test)

Statistical Analysis

All data are expressed as the mean \pm SEM or mean \pm SD, as indicated in the figure legends. Data collection and analysis were randomly assigned and performed blind to both experimental conditions and animal genotypes. Quantitative data

were statistically analyzed with Student's t -test or ANOVA with post hoc test using GraphPad Prism (version 8.0; San Diego, CA) as indicated. Statistical significance was set at $p < 0.05$. The sample size for the experiments was chosen to ensure adequate statistical power based on calculations using the G*power 3.1 software [58].

Fig. 3 *Lcn2*-deficiency attenuates the controlled cortical impact-induced brain lesion, behavioral deficit, gliosis, and proinflammatory cytokines in mice. **A** Experimental timeline. **B** Stereological quantification of the brain lesion volume in the ipsilateral hemisphere in WT and *Lcn2* KO brains at day 7 after controlled cortical impact (CCI) injury. Lesion volume was expressed as the average of brain areas between bregma -3.0 and -0.2 , normalized to respective values measured on the contralateral side ($n = 18$). Representative images (left) and quantification (right). Scale bar, 1 mm. Yellow arrows indicate ipsilateral brain. **C–D** Motor and sensory impairment in mice was measured using the pole test (C) and adhesive removal test (D), respectively, at day 6 post CCI injury. The descend time ($n = 3$) (C) and adhesive removal time ($n = 5$) (D) are shown. **E–F** Cognitive impairment in CCI mice was measured using the passive avoidance test ($n = 3$) (E), and spatial memory deficit was assessed using the Y-maze test ($n = 3$) (F), respectively, at day 6 post CCI injury. The number of alternations (left) and total arm entries (right) were compared. **G** Immunofluorescence staining revealed that GFAP and Iba-1 immunoreactivity was increased in the ipsilateral brain of WT mice at day 7 post CCI injury, whereas *Lcn2* deficiency attenuated this increase in immunoreactivity. Scale bar, 100 μm . The quantification of relative intensity of GFAP or Iba-1 is presented adjacent to the microscopic images ($n = 6$). **H** The expression levels of *Tnf* and *Il1b* mRNA in the ipsilateral brain at day 7 of CCI injury were evaluated by qPCR ($n = 3$). Results are expressed as mean \pm SEM. * $p < 0.05$ versus WT sham control groups; # $p < 0.05$ between the indicated groups; n.s., not significant (one-way ANOVA followed by Tukey's post hoc test)



Results

Traumatic Brain Injury Induces LCN2 Expression in Astrocytes

To investigate the involvement of LCN2 in TBI, we used CCI, a widely used model to study the mechanism of TBI [59] (Fig. 1A). The ipsilateral and contralateral hemispheres of the CCI brain were isolated and used for mRNA analysis. The expression of *Lcn2* mRNA was induced at day 1 in the ipsilateral brain after CCI injury in contrast to the contralateral side, and peaked at day 7 (Fig. 1B). Based on the high expression of LCN2 on day 7 after CCI injury, this condition

was used for further analyses. We conducted immunofluorescence analysis to investigate which cell types express LCN2 in CCI brain tissue. In mouse brain tissue sections, LCN2 co-localized with GFAP-positive astrocytes in the peri-contusional area (Fig. 1C) but not in neurons or microglia (Fig. S1). Overall, LCN2 protein expression also increased in the CCI brain (Fig. 1C). In addition, the mRNA levels of *Tnf* and *Il1b* were highly increased on day 7 in the CCI brain compared with the sham control (Fig. 1D).

We next evaluated LCN2 (also known as neutrophil gelatinase-associated lipocalin (NGAL) in humans) mRNA and protein expression in postmortem brain tissue of patients with CTE. RNA sequencing data revealed

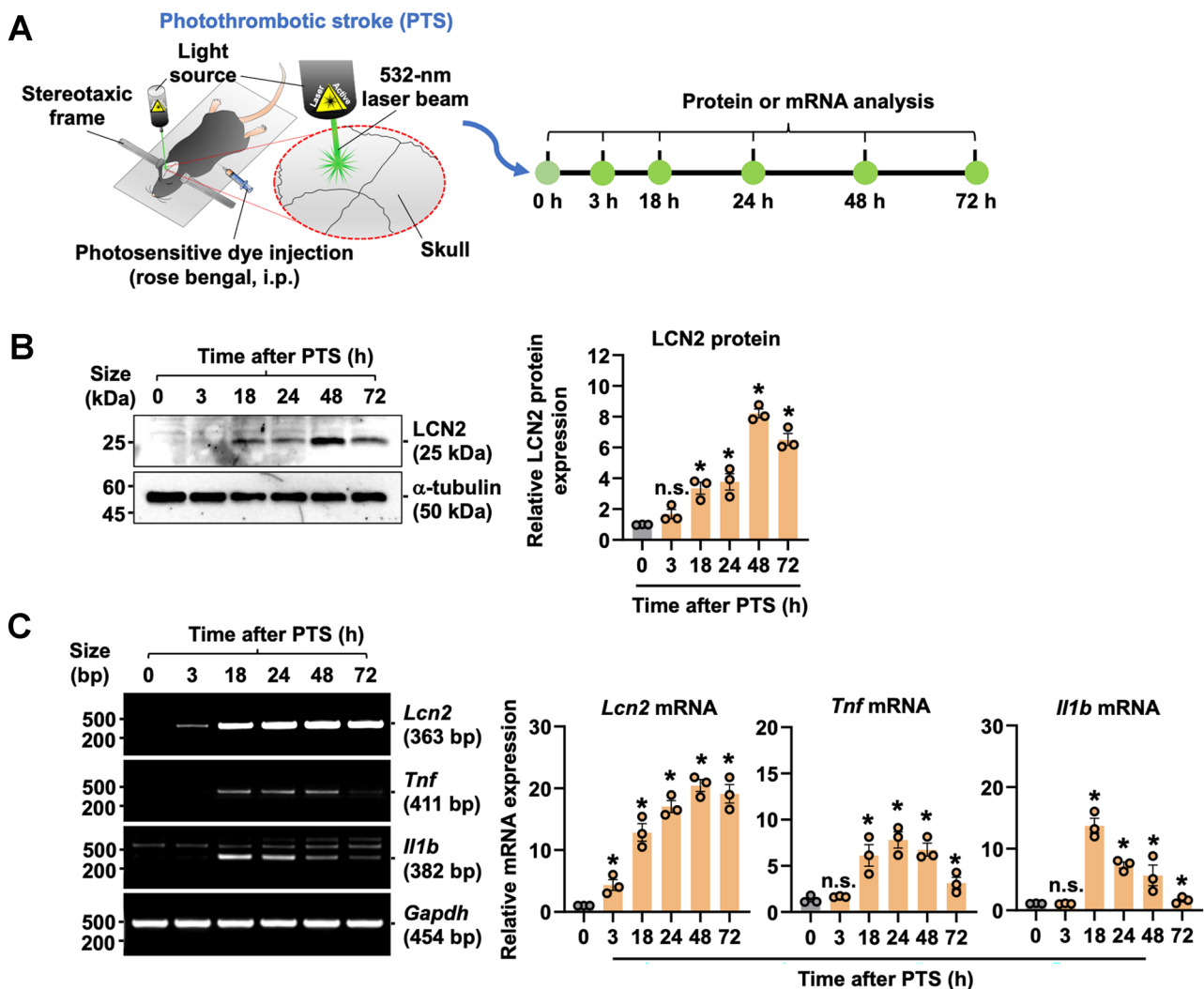


Fig. 4 Induction of LCN2 expression in the brain of photothrombotic stroke mice. **A** Experimental timeline. **B** The expressions of LCN2 protein in the ipsilateral cerebral hemisphere at 3, 18, 24, 48, and 72 h post photothrombotic stroke (PTS) were assessed by Western blot analysis. Quantification is shown in the adjacent graph ($n=3$). **C** The expression levels of *Lcn2*, *Tnf*, and *Il1b* mRNA in the brains (ipsi-

lateral hemisphere) of PTS mice were measured by conventional RT-PCR analysis. Representative gel images (left) and quantification are shown in the adjacent graph (right) ($n=3$). Results are expressed as mean \pm SEM. * $p < 0.05$ versus control (0 h) groups; n.s., not significant (one-way ANOVA followed by Tukey's post hoc test)

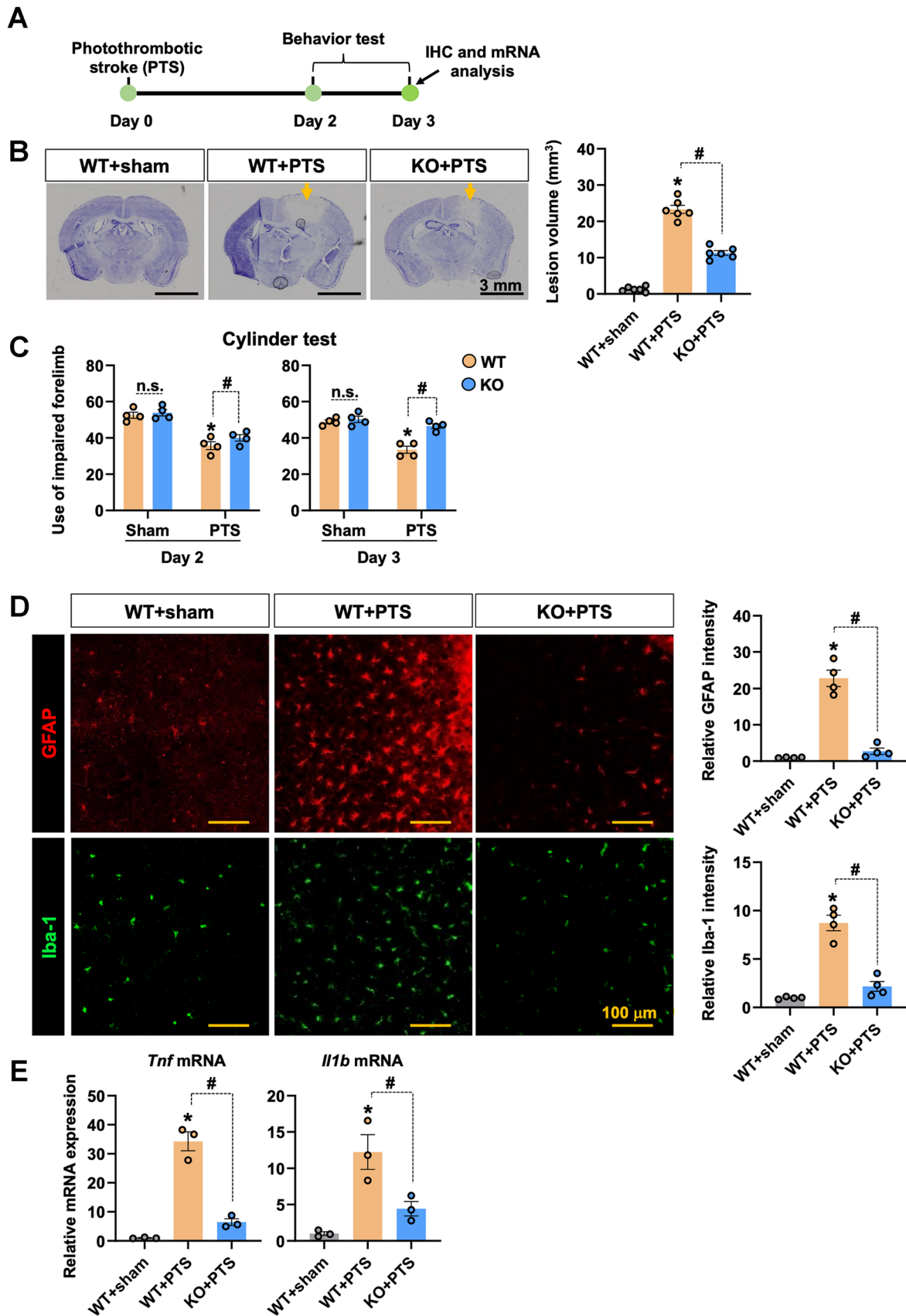


Fig. 5 *Lcn2*-deficiency attenuates the brain damage, motor function deficit, gliosis, and proinflammatory cytokines in photothrombotic stroke mice. **A** Experimental timeline. **B** Representative images of Cresyl violet-stained brain sections from WT or *Lcn2* KO mice at day 3 post photothrombotic stroke (PTS) (*left*). The quantification of brain lesion volume calculated from Cresyl violet-stained brain sections (*right*) ($n=6$). Scale bar, 3 mm. Yellow arrows indicate ipsilateral brain. **C** Motor impairment in mice was measured using the cylinder test at days 2 and 3 post PTS ($n=4$). **D** Immunofluorescence staining of GFAP and Iba-1 was increased in the ipsilateral cerebral hemisphere of WT mice at day 3 post PTS injury, whereas *Lcn2* deficiency attenuated this increase in immunoreactivity. The quantification of relative intensity of GFAP or Iba-1 is presented adjacent to the microscopic images ($n=4$). Scale bar, 100 μm . **E** The expression levels of *Tnf* and *Il1b* mRNA in the ipsilateral cerebral hemisphere at day 3 of PTS injury were evaluated by qPCR ($n=3$). Results are expressed as mean \pm SEM. * $p < 0.05$ versus WT sham control groups; # $p < 0.05$ between the indicated groups; n.s., not significant (one-way ANOVA followed by Tukey's post hoc test)

that the mRNA levels of *LCN2* were significantly increased in the postmortem brain tissue of patients with CTE (Fig. 2A). Moreover, we evaluated the expression of *LCN2* protein in the postmortem brain tissue of CTE patients [49]. Similar to the CCI animal models, significant *LCN2* protein expression was detected in reactive astrocytes and upregulated in the brains of patients with CTE (Fig. 2B). To assess the detailed morphometric characteristics of hypertrophied astrocytes, we performed Sholl analysis of astrocytes using GFAP signals. There was a significantly higher sum of intersections in cortical regions of the brain of patients with CTE than in the normal brain, indicating that reactive astrocytes have processes with more branches than the astrocytes of the normal brain (Fig. 2C). Altogether, the results indicate that *LCN2* is mainly expressed in astrocytes under TBI conditions and suggest that it may be a key contributor to secondary brain damage after TBI, considering the strong pro-inflammatory role of *LCN2* in other brain disorders [60, 61].

Role of *LCN2* in Brain Damage, Neurologic Deficit, and Neuroinflammation After TBI

To determine the contribution of *LCN2* to brain damage, subsequent motor and cognitive deficits, and neuroinflammation, both *Lcn2* KO and WT mice were subjected to CCI injury, and brain lesions were measured by Cresyl violet staining (Fig. 3A). *Lcn2* deficiency was found to reduce brain lesion volumes at day 7 after CCI (Fig. 3B) compared to WT CCI animals. In addition, the reduction in NeuN immunoreactivity (reflecting brain damage) in the peri-contusional brain region was ameliorated in *Lcn2* KO mice (Fig. S2A). Furthermore, CCI-induced motor, sensory (Fig. 3C, D), and cognitive deficits (Fig. 3E, F) were also attenuated in *Lcn2* KO mice. These observations indicate

that *LCN2* contributes to brain damage and neurological deficits following TBI.

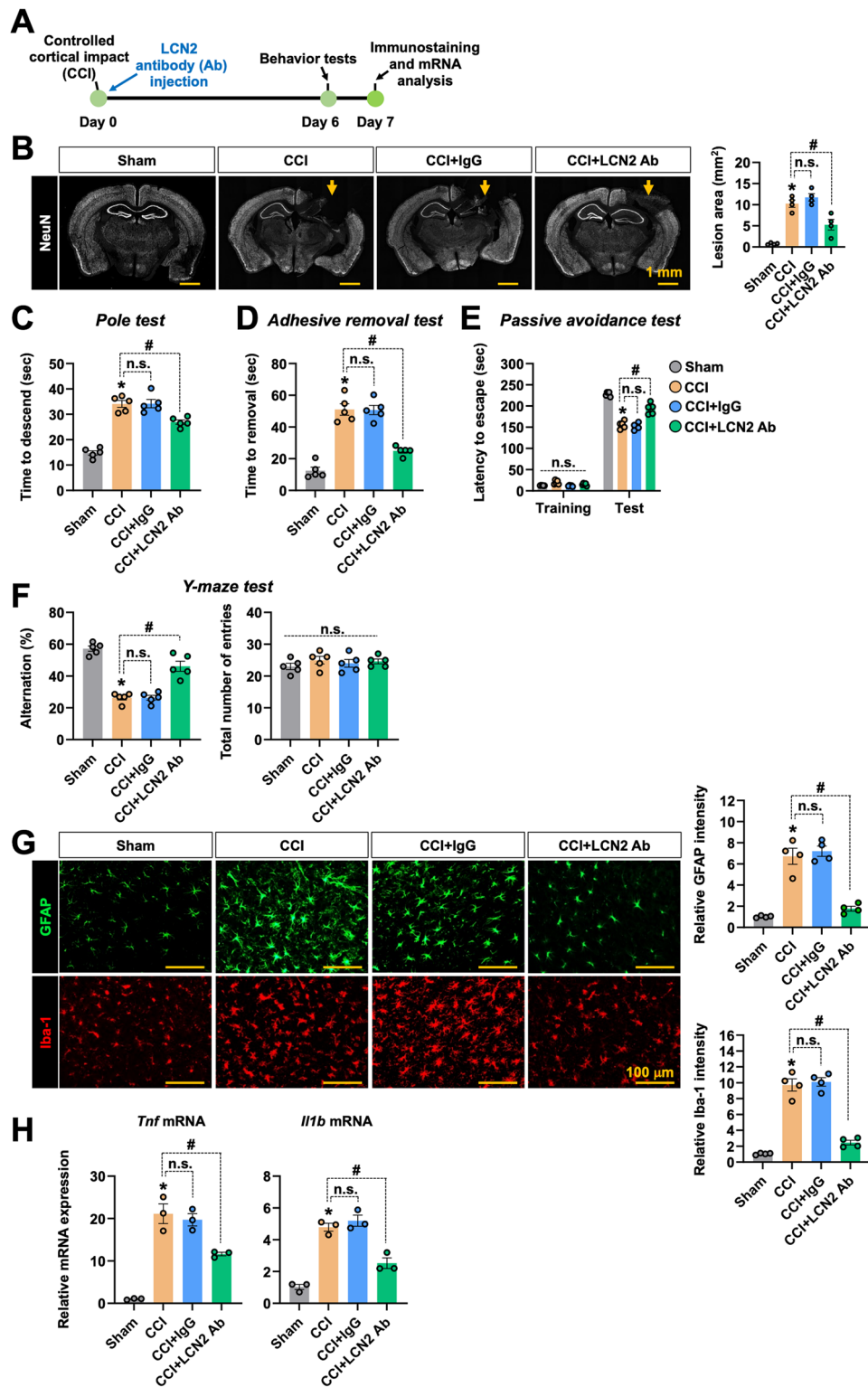
Glia activation is one of the main events involved in neuroinflammation. Immunofluorescence analyses were performed to determine the immunoreactivity of GFAP and Iba-1 in the peri-contusion area. The results indicate a heightened level of astrocytic and microglial activation under these conditions. These activated astrocytes and microglia showed hypertrophic morphology with thick processes. Importantly, such gliosis has been observed predominantly in the peri-contusional regions of the cortex (Fig. S2B) and hippocampus (Fig. 3G) of CCI mice but is reduced in *Lcn2*-deficient mice. Moreover, the CCI-induced expressions of proinflammatory cytokines, such as *Tnf* and *Il1b*, were substantially diminished by *Lcn2* deficiency (Fig. 3H). These results suggest that CCI injury-induced *LCN2* expression contributes to neuroinflammation.

Lcn2 Deficiency Attenuates Brain Damage, Behavioral Deficits, and Inflammatory Responses After Ischemic Brain Injury

We used a PTS model of ischemic brain injury to further evaluate the role of *LCN2* in secondary brain damage (Fig. 4). In humans, ischemic brain damage is observed in TBI survivors [62]. We investigated the expression of *LCN2* and inflammatory cytokines in the brains of the PTS mice (Fig. 4A). Western blot analysis of ipsilateral cerebral hemisphere revealed that *LCN2* protein expression was induced 18 h after PTS and peaked at 48 h (Fig. 4B), and proinflammatory cytokines were increased 18 h after PTS (Fig. 4C). We further examined the role of *LCN2* in PTS-induced brain injury and neuroinflammation in *Lcn2* KO mice (Fig. 5A). The *Lcn2*-deficient PTS mice showed lower levels of brain damage (Fig. 5B), motor and sensory deficits (Fig. 5C), glial activation (Fig. 5D), and proinflammatory cytokines (Fig. 5E) than WT PTS animals on day 3 after injury. These findings imply that *LCN2* plays an important role in injury-induced neuroinflammation following ischemic brain injury.

Antibody-Mediated *LCN2* Neutralization Attenuates CCI Injury-Induced Brain Damage, Behavioral Deficits, and Neuroinflammation

Since *LCN2* expression was induced in astrocytes after brain injury (Fig. 1), we explored the possibility of neutralizing brain *LCN2* as a therapeutic strategy for the prevention or treatment of secondary inflammatory brain injury in TBI. *LCN2*-neutralizing antibody was administered intracisternally to mice immediately after CCI injury, and the brain lesion area, motor and cognitive behaviors, and neuroinflammation were measured, as described in the experimental



timeline (Fig. 6A). On the ipsilateral side, CCI injury reduced NeuN immunoreactivity, and this effect was attenuated in the LCN2-neutralized mice (Fig. 6B). Control mice received an isotype control IgG injection. Notably, injection of LCN2 antibody into the CCI group significantly improved

motor and sensory abilities (Fig. 6C, D), cognitive function (Fig. 6E, F), glial activation (Figs. 6G and S3), and pro-inflammatory cytokine expression (Fig. 6H) compared to the IgG-treated CCI group. These results are consistent with those of genetic ablation of *Lcn2*.

Fig. 6 LCN2 neutralizing antibody administration ameliorates brain damage, behavioral deficit, and neuroinflammation after TBI. **A** Experimental timeline. **B** The brain lesion area in the ipsilateral hemisphere was expressed as the average of the brain area normalized to the respective values measured on the contralateral side. Representative images of controlled cortical impact (CCI) brains at day 7 after isotype control IgG or LCN2 neutralizing antibody (Ab) injection (*left*) and their quantification (*right*) ($n=4$). Scale bar, 1 mm. Yellow arrows indicate ipsilateral brain. **C–D** Motor and sensory impairment in mice was measured using the pole test (**C**) and adhesive removal test (**D**), respectively, at day 6 post CCI ($n=5$). The descend time (**C**) and adhesive removal time (**D**) are shown in the graphs. **E–F** Cognitive impairment in CCI mice was measured using the passive avoidance test (**E**) and spatial memory deficit was assessed using the Y-maze test (**F**), respectively, at day 6 post CCI ($n=5$). The number of alternations (*left*) and total arm entries (*right*) were compared. **G** Immunofluorescence analysis revealed that GFAP and Iba-1 immunoreactivity was increased in the ipsilateral brain at day 7 post CCI injury, whereas LCN2 Ab injection attenuated this increase in immunoreactivity. Scale bar, 100 μm . The quantification of relative intensity of GFAP or Iba-1 is presented adjacent to the microscopic images ($n=4$). **H** The expression levels of *Tnf* and *Il1b* mRNA in the ipsilateral brain at day 7 of CCI injury were evaluated by qPCR ($n=3$). Results are expressed as mean \pm SEM. * $p < 0.05$ versus sham control groups; # $p < 0.05$ between the indicated groups; n.s., not significant (one-way ANOVA followed by Tukey's post hoc test)

Astrocytes Secrete LCN2 to Promote Inflammatory Activation of Microglia, While Inhibiting Their Neurotrophic Effects

We used a cell scratch injury model, an *in vitro* model of TBI, to study the role of LCN2 in TBI. Scratch injury recapitulates certain aspects of TBI in that the injury is initiated by physical primary damage, followed by secondary deterioration mediated by proinflammatory cytokines released from reactive glial cells [59]. First, we confirmed cell purity in individual or co-culture of astrocytes and microglia (Fig. S4). Next, we assessed the expression of LCN2 in these cultured glial cells after scratch injury. A noticeable increase in *Lcn2* mRNA expression was observed in primary astrocytes and co-culture (astrocytes and microglia) 72 h after scratch injury, but not in primary microglia after scratch injury (Fig. 7A). These results were consistent with the results *in vivo* (Fig. 1). These results also suggest that LCN2 secreted from astrocytes may act on microglia to influence neuroinflammation in TBI.

In the next set of experiments, primary astrocytes isolated from WT or *Lcn2* KO mice were co-cultured with WT microglia to evaluate the effects of astrocyte-derived LCN2 on microglia in the scratch injury model (Fig. 7B). Scratch injury induced inflammatory cytokine expression in the co-culture of WT astrocytes and WT microglia but not in the co-culture of *Lcn2*-deficient astrocytes (KO) and WT microglia. Similarly, treatment with LCN2 antibody reduced the effect of scratch injury in the co-culture of WT astrocytes and WT microglia (Fig. 7B). These results indicate that

astrocytic LCN2 plays a critical role in microglial activation and neuroinflammation during brain injury.

Glial cell–derived neurotrophic factor (GDNF) was first characterized as a potent neurotrophic factor in neurons [63, 64]. To date, several studies have revealed the neuroprotective effects of GDNF against various toxic challenges [65]. Recently, it has been suggested that GDNF also modulates neuronal death induced by acute brain injury [66–68]. Based on these studies, we speculated a potential interaction between LCN2 and GDNF in secondary inflammatory brain injuries. First, we evaluated *Gdnf* mRNA levels in cultured astrocytes, microglia, and a co-culture of astrocytes and microglia. We found a significant increase in *Gdnf* mRNA expression in primary microglia, but not in primary astrocytes or in the co-culture following scratch injury (Fig. 8A). To further determine the role of astrocyte-derived LCN2 in scratch injury, the expressions of proinflammatory cytokines and *Gdnf* mRNA were evaluated in cultured microglial cells exposed to recombinant mouse LCN2 protein and scratch injury. Treatment of microglial cells with recombinant LCN2 protein enhanced the effects of scratch injury on the expression of *Tnf* and *Il1b* mRNA, whereas recombinant LCN2 protein reduced scratch injury–induced *Gdnf* mRNA expression (Fig. 8B). However, denatured recombinant LCN2 protein had no effect. In contrast, co-culture with *Lcn2* KO astrocytes or LCN2 antibody treatment augmented the microglial expression of *Gdnf* mRNA (Fig. 8C). These results indicate that astrocyte-derived LCN2 inhibits *Gdnf* mRNA expression in the microglia.

Finally, we evaluated *Gdnf* mRNA expression in the CCI brain. Interestingly, *Gdnf* mRNA levels were higher in *Lcn2* KO (Fig. S5A) or LCN2 antibody-injected animals (Fig. S5B) after CCI injury compared with WT mice or the control IgG-treated group. These results support the hypothesis that LCN2 negatively regulates *Gdnf* mRNA expression in brain injury.

Discussion

In this study, we investigated the role of LCN2 in the pathogenesis of TBI using the CCI and PTS rodent models. The results obtained from *in vivo* rodent models indicate that upregulation of LCN2 expression, mainly in astrocytes, plays a critical role in the secondary neuroinflammatory response to brain injury. Upregulation of LCN2 expression was also confirmed in the postmortem brain tissues of patients with CTE. Genetic ablation of *Lcn2* attenuated TBI-induced neuroinflammation as well as cognitive and motor function deficits in mice. Similarly, in cultured glial cells, astrocytic *Lcn2* deficiency lowered microglial proinflammatory cytokine expression, while elevating microglial GDNF expression following scratch injury. Altogether, our results

indicate that LCN2 is a critical mediator of neuroinflammation involved in the secondary brain damage caused by TBI. We propose dual pathological roles for astrocyte-derived LCN2 in TBI (Fig. S6): LCN2 promotes neuroinflammation through activation of microglia, and LCN2 can potentiate brain damage by inhibiting neurotrophic GDNF expression.

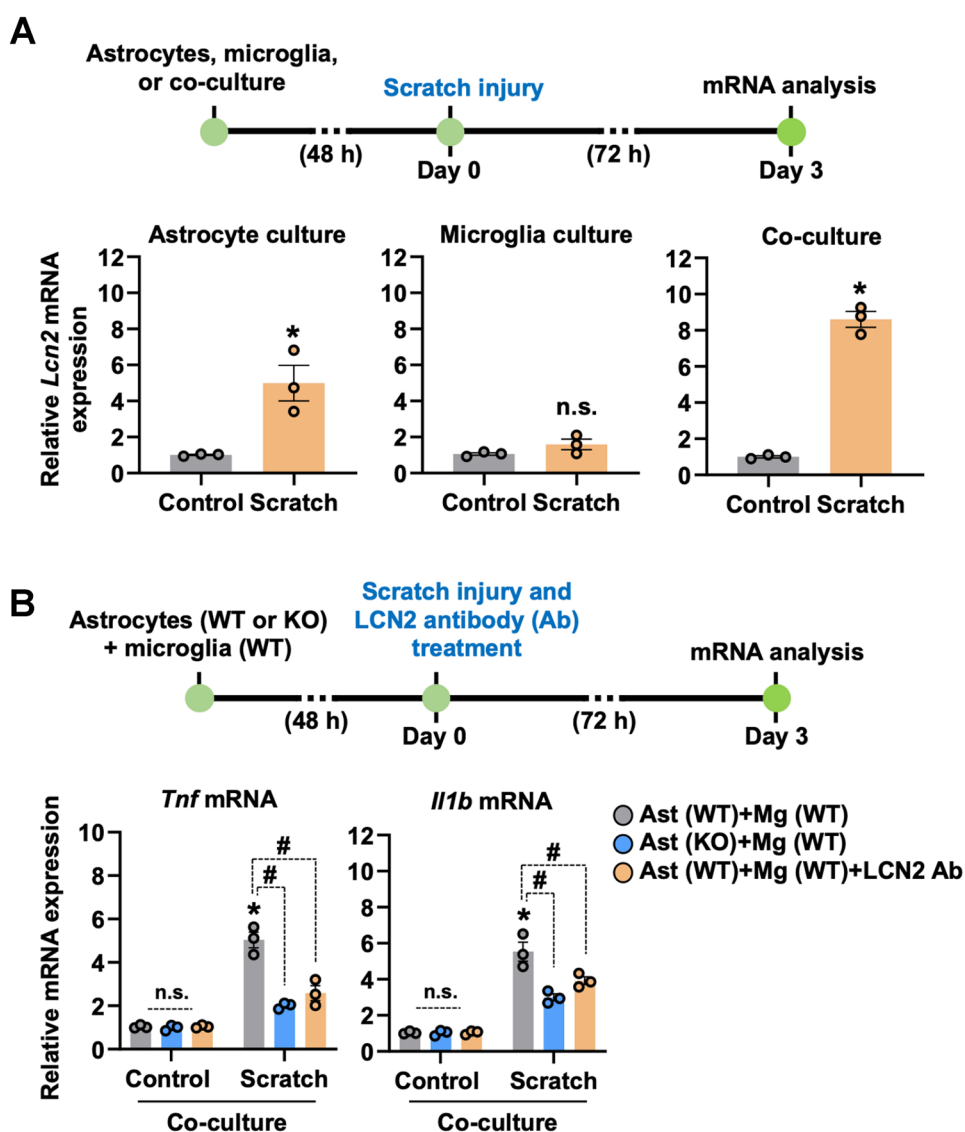
LCN2 Is a Key Regulator of Neuroinflammation in Secondary Brain Injury in TBI

Following CCI- and PTS-induced brain injury, the expression of LCN2 was significantly upregulated in the mouse brain. The unique LCN2 expression pattern in the peri-contusional brain region might correlate with the TBI pathology observed in the early phase of secondary brain injury, such as neuroinflammation. Increasing evidence suggests that secondary brain injury, particularly neuroinflammation, is a common

pathological feature of TBI [60, 69]. In addition, microglia and astrocytes following inflammatory activation play crucial roles in the pathophysiology of TBI [70]. Higher levels of astrocyte and microglial activation and proliferation have been observed in TBI-rodent models, with augmented expression of proinflammatory cytokines [60, 69, 70]. We observed that genetic deletion or antibody-mediated neutralization of LCN2 significantly reduced CCI- and PTS-induced brain damage, pro-inflammatory cytokines, glial activation, and neurological deficits. This suggests that LCN2 plays a pivotal role in inflammatory secondary brain injury following TBI.

An additional direction for this study is to look at sex differences in the role of LCN2 in the secondary inflammatory response to TBI and stroke. Most of research in the field uses male rodents, with a few research groups employing male and female rodents pooled together [71, 72]. Previous

Fig. 7 *Lcn2*-deficient astrocytes attenuates scratch injury-induced proinflammatory cytokine expression in co-culture with microglia. **A** The expression levels of *Lcn2* mRNA in the astrocytes, microglia, and co-culture (astrocyte and microglia) at 72 h after scratch injury were evaluated by qPCR ($n=3$). Results are expressed as mean \pm SEM. * $p < 0.05$ versus control groups; n.s., not significant (Student's *t*-test). **B** Astrocytes isolated from WT or *Lcn2*-deficient mice were co-cultured with WT microglia. The co-cultures were then subjected to scratch injury and LCN2 neutralizing antibody treatment, followed by mRNA analysis. The mRNA expression of *Tnf* and *Il1b* was measured using qPCR at 72 h after scratch injury ($n=3$). Ast, astrocytes; Mg, microglia. Results are expressed as mean \pm SEM. * $p < 0.05$ versus control groups; # $p < 0.05$ between the indicated groups; n.s., not significant (one-way ANOVA followed by Tukey's post hoc test)



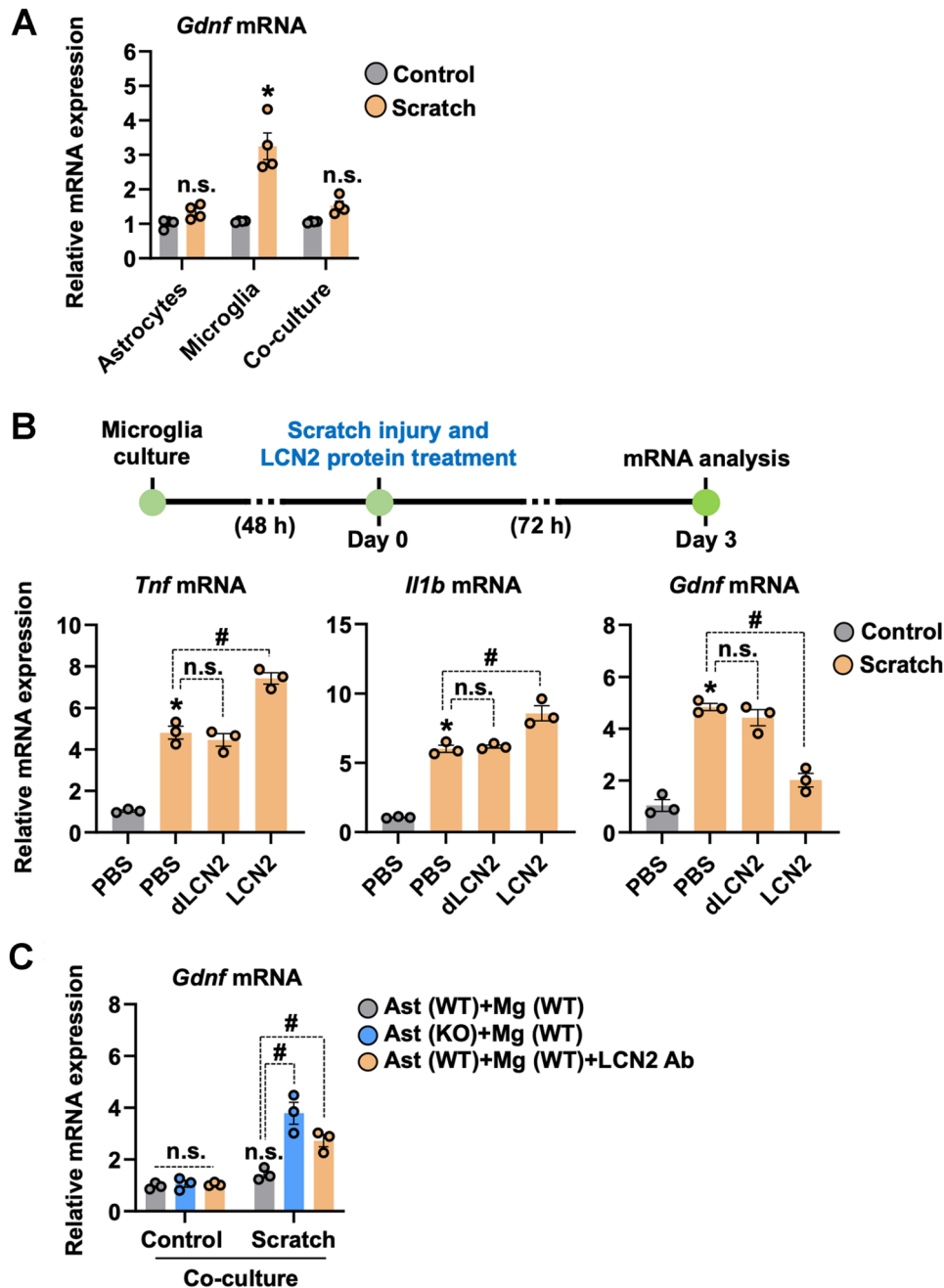


Fig. 8 LCN2 upregulates scratch injury-induced proinflammatory cytokines, while reducing GDNF levels in microglia. **A** The expression levels of *Gdnf* mRNA in the astrocytes, microglia, and co-culture (astrocyte and microglia) at 72 h after scratch injury were evaluated by qPCR ($n=4$). Results are expressed as mean \pm SEM. * $p < 0.05$ versus control groups; n.s., not significant (Student's *t*-test). **B** Primary microglia cultures were subjected to scratch injury and treatment with PBS, denatured recombinant LCN2 protein (dLCN2, 1 μ g/ml), or recombinant LCN2 protein (LCN2, 1 μ g/ml), followed by mRNA analysis. The mRNA levels of *Tnf*, *Il1b*, and *Gdnf* were determined by qPCR ($n=3$). Results are expressed as mean \pm SEM. * $p < 0.05$ versus control PBS groups (without scratch injury);

$p < 0.05$ between the indicated groups; n.s., not significant (one-way ANOVA followed by Tukey's post hoc test). **C** Astrocytes isolated from WT or *Lcn2*-deficient mice were co-cultured with WT microglia. The co-cultures were subjected to scratch injury and LCN2 neutralizing antibody (Ab) treatment, followed by mRNA analysis. The mRNA expression of *Gdnf* was measured using qPCR at 72 h after scratch injury ($n=3$). Ast, astrocytes; Mg, microglia. *Gapdh* was used as an internal control. Results are expressed as mean \pm SEM. * $p < 0.05$ versus control groups; # $p < 0.05$ between the indicated groups; n.s., not significant (one-way ANOVA followed by Tukey's post hoc test)

studies have suggested sex differences in the brain's response to injury [73–75]. It remains to be better established whether differential outcomes following brain injury in males and females are due to sex hormone differences, given the conflicting but growing body of literature documenting gender influences on injury outcome in humans and rodents [76]. It is important to recognize that human gender is not a simple binary [77, 78]; it is rather complex combinations of social and biological factors that will have to be carefully considered [79]. Because the current studies included only male animals, further research is needed to address potential gender differences in injury outcomes.

LCN2 Is a Potential Biomarker and Therapeutic Target for Secondary Brain Injury in TBI

Our TBI mouse model and CTE patient studies revealed a significant increase in LCN2 expression in injured brains. Previously, LCN2 was reported to be upregulated in the CNS of animal models of brain injury such as intracranial hemorrhage [41]. More recent animal studies have shown increased LCN2 expression in the hippocampus after lateral fluid percussion, with peak elevation at day 1 [80]. In a subsequent human trial, serum LCN2 levels increased in patients with TBI [42, 43]. These findings were partially corroborated by clinical studies in patients with stroke. A prospective study by Elneihoum et al. [81] demonstrated that LCN2 plasma levels in patients with acute ischemic cerebrovascular disease were higher than those in the control subjects. Another recent study also suggested that LCN2 could be used as a diagnostic biomarker for the injured brain [82]. As an acute-phase protein, LCN2 expression is highly induced during the early phases of brain injury. These reports strongly indicate that LCN2 is a promising biomarker of brain injury. When combined with other existing or new biomarkers, the detection of LCN2 protein can facilitate the diagnosis or prognosis of secondary brain injury in TBI patients.

Our results, based on *Lcn2* KO mice and a neutralizing antibody against LCN2, suggest that LCN2 is a potential therapeutic target in TBI. LCN2 targeting may have a wide applicability in multiple CNS disorders. Preclinical studies have shown that LCN2 deficiency markedly decreases neuroinflammation in mouse models of hemorrhagic and ischemic stroke [40, 41, 83, 84], spinal cord injury [85], and experimental autoimmune encephalomyelitis [34]. These findings suggest that LCN2 is a critical mediator of neuroinflammation in various CNS disorders. Neutralization of LCN2 using LCN2 antibody may inhibit or reverse neuroinflammatory responses in CNS disorders [25]. Although neutralizing the activity of extracellular LCN2 protein by LCN2 antibody was used in the current study, other therapeutic approaches that inhibit the expression and secretion of LCN2 [86], or interfere with the interaction between

LCN2 and its receptors [87], are also potential avenues for therapeutic development [25]. In this study, however, the interventions were either prior to (genetic manipulation) or immediately after the injury (neutralizing antibody). As several interventions with a restricted therapeutic window have previously failed in a clinical setting, further studies are required to address the therapeutic window of LCN2 inhibition. Moreover, in the current study, therapeutic behavioral effects of LCN2 inhibition were evaluated in a relatively short time period after brain injury; thus, additional studies are necessary to test long-term effects of LCN2 inhibition.

LCN2 Inhibition of Microglial Neurotrophic Activity in TBI

Our results show that LCN2 significantly decreases *Gdnf* mRNA levels in microglia, suggesting the involvement of LCN2 in the modulation of microglial neurotrophic and neuroprotective activities in TBI. GDNF produced by activated microglia/macrophages can lead to that reparation of CNS injuries. After striatal mechanical injury [88, 89] and spinal cord injury [90], activated microglia/macrophages express GDNF, thereby inducing axonal sprouting and locomotor improvements. Indeed, the inhibition of GDNF expression using antisense oligonucleotides drastically reduced axonal sprouting [91]. In addition, GDNF delivery based on transduced hematopoietic stem cell transplantation successfully rescued nigral dopaminergic neurons and improved motor function in a Parkinson's disease mouse model [92, 93]. GDNF has also been linked to the survival of dopaminergic cells in the substantia nigra through an increase in synaptic excitability [94] and the inhibition of apoptosis [95]. Thus, LCN2 inhibition of microglial GDNF may be another mechanism of inflammatory secondary injury in TBI.

Conclusion

Our study demonstrated that LCN2 is expressed and released predominantly by reactive astrocytes in response to TBI, thus acting as a neuroinflammatory mediator in secondary injury. Once released, LCN2 mediates neuroinflammation by inducing proinflammatory microglial activation. Our data also suggest an important role for LCN2 in suppressing the microglial expression of neurotrophic factors after TBI. The detrimental role of LCN2 after TBI was corroborated by studies using *Lcn2* KO mice and neutralizing antibodies. Taken together, astrocytic LCN2 may play a pivotal role as an intrinsic promoter of neuroinflammation in TBI by triggering proinflammatory microglial activation while inhibiting their neurotrophic effects. Thus, LCN2 could be exploited as a biomarker and therapeutic target for secondary injuries in TBI.

Supplementary Information The online version contains supplementary material available at <https://doi.org/10.1007/s13311-022-01333-5>.

Required Author Forms Disclosure forms provided by the authors are available with the online version of this article.

Author Contribution J.H.K. and R.J.K. performed the research and analyzed the data. S.J.H. and H.R. performed the immunostaining of human CTE brain and analyzed the data. H.J. and Y.B. contributed to controlled cortical impact surgery. J.H.K. contributed to photothrombotic stroke surgery. J.H.K. and K.S. designed the study. J.H.K. and K.S. wrote the manuscript, and all authors critically reviewed the text and figures. All authors have read and approved the final manuscript.

Funding This work was supported by National Research Foundation of Korea (NRF) grants funded by the Korean government (NRF-2017R1A5A2015391 and 2020M3E5D9079764).

Data Availability The datasets generated and/or analyzed during this study are available from the corresponding author upon reasonable request.

Declarations

Ethics Approval and Consent to Participate The current study was approved by the appropriate local ethics committee. Informed consent was procured from all human participants or their caregivers who donated their tissue. All animal experiments were performed in accordance with approved animal protocols and guidelines established by the Animal Care Committee of Kyungpook National University (No. KNU 2022-0290).

Conflict of Interest The authors declare no competing interests.

References

1. Khellaf A, Khan DZ, Helmy A. Recent advances in traumatic brain injury. *J Neurol*. 2019;266:2878–89.
2. O’Leary RA, Nichol AD. Pathophysiology of severe traumatic brain injury. *J Neurosurg Sci*. 2018;62:542–8.
3. Taylor CA, Bell JM, Breiding MJ, Xu L. Traumatic brain injury-related emergency department visits, hospitalizations, and deaths - United States, 2007 and 2013. *MMWR Surveill Summ*. 2017;66:1–16.
4. Selassie AW, Zaloshnja E, Langlois JA, Miller T, Jones P, Steiner C. Incidence of long-term disability following traumatic brain injury hospitalization, United States, 2003. *J Head Trauma Rehabil*. 2008;23:123–31.
5. Barnes DE, Byers AL, Gardner RC, Seal KH, Boscardin WJ, Yaffe K. Association of mild traumatic brain injury with and without loss of consciousness with dementia in US military veterans. *JAMA Neurol*. 2018;75:1055–61.
6. Alway Y, Gould KR, Johnston L, McKenzie D, Ponsford J. A prospective examination of Axis I psychiatric disorders in the first 5 years following moderate to severe traumatic brain injury. *Psychol Med*. 2016;46:1331–41.
7. Whelan-Goodinson R, Ponsford J, Johnston L, Grant F. Psychiatric disorders following traumatic brain injury: their nature and frequency. *J Head Trauma Rehabil*. 2009;24:324–32.
8. Crane PK, Gibbons LE, Dams-O’Connor K, Trittschuh E, Leverenz JB, Keene CD, et al. Association of traumatic brain injury with late-life neurodegenerative conditions and neuropathologic findings. *JAMA Neurol*. 2016;73:1062–9.
9. McKee AC, Daneshvar DH, Alvarez VE, Stein TD. The neuropathology of sport. *Acta Neuropathol*. 2014;127:29–51.
10. Hong YT, Veenith T, Dewar D, Outtrim JG, Mani V, Williams C, et al. Amyloid imaging with carbon 11-labeled Pittsburgh compound B for traumatic brain injury. *JAMA Neurol*. 2014;71:23–31.
11. VanItallie TB. Traumatic brain injury (TBI) in collision sports: possible mechanisms of transformation into chronic traumatic encephalopathy (CTE). *Metabolism*. 2019;100S:153943.
12. Coughlin JM, Wang Y, Minn I, Bienko N, Ambinder EB, Xu X, et al. Imaging of glial cell activation and white matter integrity in brains of active and recently retired national football league players. *JAMA Neurol*. 2017;74:67–74.
13. Cherry JD, Tripodis Y, Alvarez VE, Huber B, Kiernan PT, Daneshvar DH, et al. Microglial neuroinflammation contributes to tau accumulation in chronic traumatic encephalopathy. *Acta Neuropathol Commun*. 2016;4:112.
14. Ramlackhansingh AF, Brooks DJ, Greenwood RJ, Bose SK, Turkheimer FE, Kinnunen KM, et al. Inflammation after trauma: microglial activation and traumatic brain injury. *Ann Neurol*. 2011;70:374–83.
15. Kaur P, Sharma S. Recent advances in pathophysiology of traumatic brain injury. *Curr Neuropharmacol*. 2018;16:1224–38.
16. Liston A, Korn T. Gene delivery of interleukin 2 treats neuro-inflammation in traumatic brain injury. *Nat Immunol*. 2022;23:834–5.
17. Dixon KJ. Pathophysiology of traumatic brain injury. *Phys Med Rehabil Clin N Am*. 2017;28:215–25.
18. Xiong Y, Mahmood A, Chopp M. Current understanding of neuroinflammation after traumatic brain injury and cell-based therapeutic opportunities. *Chin J Traumatol*. 2018;21:137–51.
19. Kumar A, Stoica BA, Loane DJ, Yang M, Abulwerdi G, Khan N, et al. Microglial-derived microparticles mediate neuroinflammation after traumatic brain injury. *J Neuroinflammation*. 2017;14:47.
20. Kumar A, Loane DJ. Neuroinflammation after traumatic brain injury: opportunities for therapeutic intervention. *Brain Behav Immun*. 2012;26:1191–201.
21. Morganti-Kossmann MC, Satgunaseelan L, Bye N, Kossmann T. Modulation of immune response by head injury. *Injury*. 2007;38:1392–400.
22. Davalos D, Grutzendler J, Yang G, Kim JV, Zuo Y, Jung S, et al. ATP mediates rapid microglial response to local brain injury in vivo. *Nat Neurosci*. 2005;8:752–8.
23. Block ML, Zecca L, Hong JS. Microglia-mediated neurotoxicity: uncovering the molecular mechanisms. *Nat Rev Neurosci*. 2007;8:57–69.
24. Zhang D, Hu X, Qian L, O’Callaghan JP, Hong JS. Astrogliosis in CNS pathologies: is there a role for microglia? *Mol Neurobiol*. 2010;41:232–41.
25. Suk K. Lipocalin-2 as a therapeutic target for brain injury: an astrocentric perspective. *Prog Neurobiol*. 2016;144:158–72.
26. Ferreira AC, Da Mesquita S, Sousa JC, Correia-Neves M, Sousa N, Palha JA, et al. From the periphery to the brain: lipocalin-2, a friend or foe? *Prog Neurobiol*. 2015;131:120–36.
27. Jang E, Kim JH, Lee S, Kim JH, Seo JW, Jin M, et al. Phenotypic polarization of activated astrocytes: the critical role of lipocalin-2 in the classical inflammatory activation of astrocytes. *J Immunol*. 2013;191:5204–19.
28. Jang E, Lee S, Kim JH, Kim JH, Seo JW, Lee WH, et al. Secreted protein lipocalin-2 promotes microglial M1 polarization. *FASEB J*. 2013;27:1176–90.
29. Lee S, Lee WH, Lee MS, Mori K, Suk K. Regulation by lipocalin-2 of neuronal cell death, migration, and morphology. *J Neurosci Res*. 2012;90:540–50.
30. Lee S, Park JY, Lee WH, Kim H, Park HC, Mori K, et al. Lipocalin-2 is an autocrine mediator of reactive astrocytosis. *J Neurosci*. 2009;29:234–49.

31. Lee S, Lee J, Kim S, Park JY, Lee WH, Mori K, et al. A dual role of lipocalin 2 in the apoptosis and deramification of activated microglia. *J Immunol*. 2007;179:3231–41.
32. Lee S, Kim JH, Kim JH, Seo JW, Han HS, Lee WH, et al. Lipocalin-2 Is a chemokine inducer in the central nervous system: role of chemokine ligand 10 (CXCL10) in lipocalin-2-induced cell migration. *J Biol Chem*. 2011;286:43855–70.
33. Bi F, Huang C, Tong J, Qiu G, Huang B, Wu Q, et al. Reactive astrocytes secrete lcn2 to promote neuron death. *Proc Natl Acad Sci U S A*. 2013;110:4069–74.
34. Nam Y, Kim JH, Seo M, Kim JH, Jin M, Jeon S, et al. Lipocalin-2 protein deficiency ameliorates experimental autoimmune encephalomyelitis: the pathogenic role of lipocalin-2 in the central nervous system and peripheral lymphoid tissues. *J Biol Chem*. 2014;289:16773–89.
35. Jha MK, Jeon S, Jin M, Ock J, Kim JH, Lee WH, et al. The pivotal role played by lipocalin-2 in chronic inflammatory pain. *Exp Neurol*. 2014;254:41–53.
36. Jeon S, Jha MK, Ock J, Seo J, Jin M, Cho H, et al. Role of lipocalin-2-chemokine axis in the development of neuropathic pain following peripheral nerve injury. *J Biol Chem*. 2013;288:24116–27.
37. Naude PJ, Nyakas C, Eiden LE, Ait-Ali D, van der Heide R, Engelborghs S, et al. Lipocalin 2: novel component of proinflammatory signaling in Alzheimer's disease. *FASEB J*. 2012;26:2811–23.
38. Kim BW, Jeong KH, Kim JH, Jin M, Kim JH, Lee MG, et al. Pathogenic upregulation of glial lipocalin-2 in the Parkinsonian dopaminergic system. *J Neurosci*. 2016;36:5608–22.
39. Kim JH, Ko PW, Lee HW, Jeong JY, Lee MG, Kim JH, et al. Astrocyte-derived lipocalin-2 mediates hippocampal damage and cognitive deficits in experimental models of vascular dementia. *Glia*. 2017;65:1471–90.
40. Jin M, Kim JH, Jang E, Lee YM, Soo Han H, Woo DK, et al. Lipocalin-2 deficiency attenuates neuroinflammation and brain injury after transient middle cerebral artery occlusion in mice. *J Cereb Blood Flow Metab*. 2014;34:1306–14.
41. Dong M, Xi G, Keep RF, Hua Y. Role of iron in brain lipocalin 2 upregulation after intracerebral hemorrhage in rats. *Brain Res*. 2013;1505:86–92.
42. Shen LJ, Zhou J, Guo M, Yang CS, Xu QC, Lv QW, et al. Serum lipocalin-2 concentrations and mortality of severe traumatic brain injury. *Clin Chim Acta*. 2017;474:130–5.
43. Zhao J, Chen H, Zhang M, Zhang Y, Qian C, Liu Y, et al. Early expression of serum neutrophil gelatinase-associated lipocalin (NGAL) is associated with neurological severity immediately after traumatic brain injury. *J Neurol Sci*. 2016;368:392–8.
44. Chen Y, Mao H, Yang KH, Abel T, Meaney DF. A modified controlled cortical impact technique to model mild traumatic brain injury mechanics in mice. *Front Neurol*. 2014;5:100.
45. Livak KJ, Schmittgen TD. Analysis of relative gene expression data using real-time quantitative PCR and the 2(-Delta Delta C(T)) Method. *Methods*. 2001;25:402–8.
46. Mez J, Solomon TM, Daneshvar DH, Murphy L, Kiernan PT, Montenigro PH, et al. Assessing clinicopathological correlation in chronic traumatic encephalopathy: rationale and methods for the UNITE study. *Alzheimers Res Ther*. 2015;7:62.
47. Vonsattel JP, Amaya Mdel P, Cortes EP, Mancevska K, Keller CE. Twenty-first century brain banking: practical prerequisites and lessons from the past: the experience of New York Brain Bank, Taub Institute, Columbia University. *Cell Tissue Bank*. 2008;9:247–58.
48. Lee J, Kim Y, Liu T, Hwang YJ, Hyeon SJ, Im H, et al. SIRT3 deregulation is linked to mitochondrial dysfunction in Alzheimer's disease. *Aging Cell*. 2018;17:e12679.
49. Seo JS, Lee S, Shin JY, Hwang YJ, Cho H, Yoo SK, et al. Transcriptome analyses of chronic traumatic encephalopathy show alterations in protein phosphatase expression associated with tauopathy. *Exp Mol Med*. 2017;49:e333.
50. Abe K, Taguchi K, Wasai T, Ren J, Utsunomiya I, Shinohara T, et al. Biochemical and pathological study of endogenous 1-benzyl-1,2,3,4-tetrahydroisoquinoline-induced parkinsonism in the mouse. *Brain Res*. 2001;907:134–8.
51. Bouet V, Boulovard M, Toutain J, Divoux D, Bernaudin M, Schumann-Bard P, et al. The adhesive removal test: a sensitive method to assess sensorimotor deficits in mice. *Nat Protoc*. 2009;4:1560–4.
52. Sarnyai Z, Sibille EL, Pavlides C, Fenster RJ, McEwen BS, Toth M. Impaired hippocampal-dependent learning and functional abnormalities in the hippocampus in mice lacking serotonin(1A) receptors. *Proc Natl Acad Sci U S A*. 2000;97:14731–6.
53. Eagle AL, Wang H, Robison AJ. Sensitive assessment of hippocampal learning using temporally dissociated passive avoidance task. *Bio Protoc*. 2016;6:e1821.
54. Mendes-Pinheiro B, Soares-Cunha C, Marote A, Loureiro-Campos E, Campos J, Barata-Antunes S, et al. Unilateral intrastriatal 6-hydroxydopamine lesion in mice: a closer look into non-motor phenotype and glial response. *Int J Mol Sci*. 2021;22:11530.
55. Choi IS, Kim JH, Jeong JY, Lee MG, Suk K, Jang IS. Astrocyte-derived adenosine excites sleep-promoting neurons in the ventrolateral preoptic nucleus: astrocyte-neuron interactions in the regulation of sleep. *Glia*. 2022;70:1864–85.
56. Saura J, Tusell JM, Serratos J. High-yield isolation of murine microglia by mild trypsinization. *Glia*. 2003;44:183–9.
57. Gao K, Wang CR, Jiang F, Wong AY, Su N, Jiang JH, et al. Traumatic scratch injury in astrocytes triggers calcium influx to activate the JNK/c-Jun/AP-1 pathway and switch on GFAP expression. *Glia*. 2013;61:2063–77.
58. Faul F, Erdfelder E, Lang AG, Buchner A. G*Power 3: a flexible statistical power analysis program for the social, behavioral, and biomedical sciences. *Behav Res Methods*. 2007;39:175–91.
59. Osier ND, Dixon CE. The controlled cortical impact model: applications, considerations for researchers, and future directions. *Front Neurol*. 2016;7:134.
60. Simon DW, McGeachy MJ, Bayir H, Clark RS, Loane DJ, Kochanek PM. The far-reaching scope of neuroinflammation after traumatic brain injury. *Nat Rev Neurol*. 2017;13:171–91.
61. Crowley MG, Liska MG, Borlongan CV. Stem cell therapy for sequestering neuroinflammation in traumatic brain injury: an update on exosome-targeting to the spleen. *J Neurosurg Sci*. 2017;61:291–302.
62. Kowalski RG, Haarbauer-Krupa JK, Bell JM, Corrigan JD, Hammond FM, Torbey MT, et al. Acute ischemic stroke after moderate to severe traumatic brain injury: incidence and impact on outcome. *Stroke*. 2017;48:1802–9.
63. Henderson CE, Phillips HS, Pollock RA, Davies AM, Lemeulle C, Armanini M, et al. GDNF: a potent survival factor for motoneurons present in peripheral nerve and muscle. *Science*. 1994;266:1062–4.
64. Lin LF, Doherty DH, Lile JD, Bektesh S, Collins F. GDNF: a glial cell line-derived neurotrophic factor for midbrain dopaminergic neurons. *Science*. 1993;260:1130–2.
65. Kriegstein K, Suter-Crazzolara C, Fischer WH, Unsicker K. TGF-beta superfamily members promote survival of midbrain dopaminergic neurons and protect them against MPP+ toxicity. *EMBO J*. 1995;14:736–42.
66. Kotliarova A, Sidorova YA. Glial cell line-derived neurotrophic factor family ligands, players at the interface of neuroinflammation and neuroprotection: focus onto the glia. *Front Cell Neurosci*. 2021;15:679034.
67. Wang J, Yang Z, Liu C, Zhao Y, Chen Y. Activated microglia provide a neuroprotective role by balancing glial cell-line derived neurotrophic factor and tumor necrosis factor-alpha secretion after subacute cerebral ischemia. *Int J Mol Med*. 2013;31:172–8.

68. Wang Y, Lin SZ, Chiou AL, Williams LR, Hoffer BJ. Glial cell line-derived neurotrophic factor protects against ischemia-induced injury in the cerebral cortex. *J Neurosci*. 1997;17:4341–8.
69. Jassam YN, Izzy S, Whalen M, McGavern DB, El Khoury J. Neuroimmunology of traumatic brain injury: time for a paradigm shift. *Neuron*. 2017;95:1246–65.
70. Chiu CC, Liao YE, Yang LY, Wang JY, Tweedie D, Karnati HK, et al. Neuroinflammation in animal models of traumatic brain injury. *J Neurosci Methods*. 2016;272:38–49.
71. Villasana LE, Peters A, McCallum R, Liu C, Schnell E. Diazepam inhibits post-traumatic neurogenesis and blocks aberrant dendritic development. *J Neurotrauma*. 2019;36:2454–67.
72. Yu TS, Kim A, Kernie SG. Donepezil rescues spatial learning and memory deficits following traumatic brain injury independent of its effects on neurogenesis. *PLoS ONE*. 2015;10:e0118793.
73. Newell EA, Todd BP, Luo Z, Evans LP, Ferguson PJ, Bassuk AG. A mouse model for juvenile, lateral fluid percussion brain injury reveals sex-dependent differences in neuroinflammation and functional recovery. *J Neurotrauma*. 2020;37:635–46.
74. Rahimian R, Cordeau P Jr, Kriz J. Brain response to injuries: when microglia go sexist. *Neuroscience*. 2019;405:14–23.
75. Acaz-Fonseca E, Duran JC, Carrero P, Garcia-Segura LM, Arevalo MA. Sex differences in glia reactivity after cortical brain injury. *Glia*. 2015;63:1966–81.
76. Gupte R, Brooks W, Vukas R, Pierce J, Harris J. Sex differences in traumatic brain injury: what we know and what we should know. *J Neurotrauma*. 2019;36:3063–91.
77. Joel D. Beyond the binary: rethinking sex and the brain. *Neurosci Biobehav Rev*. 2021;122:165–75.
78. Ainsworth C. Sex redefined. *Nature*. 2015;518:288–91.
79. Giordano KR, Rojas-Valencia LM, Bhargava V, Lifshitz J. Beyond binary: influence of sex and gender on outcome after traumatic brain injury. *J Neurotrauma*. 2020;37:2454–9.
80. Zhao J, Xi G, Wu G, Keep RF, Hua Y. Deferoxamine attenuated the upregulation of lipocalin-2 induced by traumatic brain injury in rats. *Acta Neurochir Suppl*. 2016;121:291–4.
81. Elneihoum AM, Falke P, Axelsson L, Lundberg E, Lindgarde F, Ohlsson K. Leukocyte activation detected by increased plasma levels of inflammatory mediators in patients with ischemic cerebrovascular diseases. *Stroke*. 1996;27:1734–8.
82. Abella V, Scotece M, Conde J, Gomez R, Lois A, Pino J, et al. The potential of lipocalin-2/NGAL as biomarker for inflammatory and metabolic diseases. *Biomarkers*. 2015;20:565–71.
83. Ni W, Zheng M, Xi G, Keep RF, Hua Y. Role of lipocalin-2 in brain injury after intracerebral hemorrhage. *J Cereb Blood Flow Metab*. 2015;35:1454–61.
84. Egashira Y, Hua Y, Keep RF, Xi G. Acute white matter injury after experimental subarachnoid hemorrhage: potential role of lipocalin 2. *Stroke*. 2014;45:2141–3.
85. Rathore KI, Berard JL, Redensek A, Chierzi S, Lopez-Vales R, Santos M, et al. Lipocalin 2 plays an immunomodulatory role and has detrimental effects after spinal cord injury. *J Neurosci*. 2011;31:13412–9.
86. Cowland JB, Muta T, Borregaard N. IL-1beta-specific up-regulation of neutrophil gelatinase-associated lipocalin is controlled by IkappaB-zeta. *J Immunol*. 2006;176:5559–66.
87. Devireddy LR, Gazin C, Zhu X, Green MR. A cell-surface receptor for lipocalin 24p3 selectively mediates apoptosis and iron uptake. *Cell*. 2005;123:1293–305.
88. Batchelor PE, Porritt MJ, Martinello P, Parish CL, Liberatore GT, Donnan GA, et al. Macrophages and microglia produce local trophic gradients that stimulate axonal sprouting toward but not beyond the wound edge. *Mol Cell Neurosci*. 2002;21:436–53.
89. Batchelor PE, Liberatore GT, Wong JY, Porritt MJ, Frerichs F, Donnan GA, et al. Activated macrophages and microglia induce dopaminergic sprouting in the injured striatum and express brain-derived neurotrophic factor and glial cell line-derived neurotrophic factor. *J Neurosci*. 1999;19:1708–16.
90. Hashimoto M, Nitta A, Fukumitsu H, Nomoto H, Shen L, Furukawa S. Inflammation-induced GDNF improves locomotor function after spinal cord injury. *NeuroReport*. 2005;16:99–102.
91. Batchelor PE, Liberatore GT, Porritt MJ, Donnan GA, Howells DW. Inhibition of brain-derived neurotrophic factor and glial cell line-derived neurotrophic factor expression reduces dopaminergic sprouting in the injured striatum. *Eur J Neurosci*. 2000;12:3462–8.
92. Chen C, Guderyon MJ, Li Y, Ge G, Bhattacharjee A, Ballard C, et al. Non-toxic HSC transplantation-based macrophage/microglia-mediated GDNF delivery for Parkinson's disease. *Mol Ther Methods Clin Dev*. 2020;17:83–98.
93. Chen C, Li X, Ge G, Liu J, Biju KC, Laing SD, et al. GDNF-expressing macrophages mitigate loss of dopamine neurons and improve Parkinsonian symptoms in MitoPark mice. *Sci Rep*. 2018;8:5460.
94. Bourque MJ, Trudeau LE. GDNF enhances the synaptic efficacy of dopaminergic neurons in culture. *Eur J Neurosci*. 2000;12:3172–80.
95. Burke RE, Antonelli M, Sulzer D. Glial cell line-derived neurotrophic growth factor inhibits apoptotic death of postnatal substantia nigra dopamine neurons in primary culture. *J Neurochem*. 1998;71:517–25.

Publisher's Note Springer Nature remains neutral with regard to jurisdictional claims in published maps and institutional affiliations.

Springer Nature or its licensor (e.g. a society or other partner) holds exclusive rights to this article under a publishing agreement with the author(s) or other rightsholder(s); author self-archiving of the accepted manuscript version of this article is solely governed by the terms of such publishing agreement and applicable law.